Desalination and Water Treatment
www.deswater.com

doi:10.5004/dwt.2017.20696

76 (2017) 30–39
May

Soft computing method for modeling and optimization of air and water gap membrane distillation — a genetic programming approach

Akbar Asadi Tashvigh, Bahram Nasernejad*

Department of Chemical Engineering, Amirkabir University of Technology, No. 424, Hafez Ave., Tehran, Iran, Tel. +98-9358748465, email: akbar.asadi@aut.ac.ir (A. Asadi Tashvigh), Tel. +98-2164543199, email: banana@aut.ac.ir (B. Nasernejad)

Received 18 October 2016; Accepted 12 March 2017

ABSTRACT

An empirical genetic programming (GP) model is developed to predict the performance of air and water gap membrane distillation (AGMD and WGMD) processes. Feed temperature, T_f, feed concentration, C_{feed}, feed flow rate, Q_f, and coolant flow rate, Q_c, were considered as input parameters, and the permeate flux was considered to be the output. The gap width is kept constant for both configurations (AGMD and WGMD) so the comparison between these two designs is based on the fixed gap width. In order to evaluate the accuracy of model, the effects of operating factors on the permeate flux were studied and compared to the experimental data. Moreover, some statistical analysis was done and exhibited a good agreement between predicated and experimental results. Using the obtained model, the impact of different variables on the process performance calculated and it was found that T_f, has the most important effect on the process performance. Finally, the optimum conditions were found by Genetic Algorithm (GA) as: Q_f = 4.512 L/min, C_{feed} = 0.145 g/L, T_f = 90°C, Q_c = 3.132 L/min with a maximum permeate flux of 38.972 L/m² h and 83.621 L/m² h for AGMD and WGMD, respectively.

Keywords: Membrane distillation; Air and water gaps; Genetic programming; Optimization

1. Introduction

As time goes by, the existence and supply of fresh water for the human population on planet earth will become an issue of great magnitude due to the scarcity of it [1–3]. More countries, especially those with already limited access to freshwater resources, such as those in the Middle East which only has access to less than 1% of the total existing global drinkable water per capita, will be exposed to more serious problems [4]. Therefore, one of the strategic options to satisfy the current and future request for freshwater in countries established around the Persian Gulf is to build up desalination units which hence causes the immediate need to construct economic units for water desalination to arise. Nowadays, it has been proved that membrane separation processes have several advantages for desalination and water reuse of contaminated resources, in comparison to the conventional separation methods [5–9]. Membrane distillation, which is a thermally driven separation process has emerged particularly for desalination. A hydrophobic membrane as a contactor media separates two fluids kept at different temperatures where the separation is obtained by the mass transfer of the pure vapor [10–12]. The partial vapor pressure difference of sides of membrane which is caused by the temperature difference is the driving force of the process [1,13–16]. Significant benefits of MD includes: a very low effect of feed concentration on the desalination performance, and the theoretical ability to reach 100% salt rejection [1,13,17,18]. Typically, there are four types of membranes arrangements for MD process: vacuum membrane distillation (VMD), air gap membrane distillation (AGMD), direct or water contact membrane distillation (DCMD or WGMD), and the sweeping gas membrane distillation (SGMD) [17,19,20]. AGMD configuration is appropriate for water desalination [21], on the other hand water gap has exhibited a higher efficiency and less heat loss in comparison to AGMD [17,22,23]. Therefore, these two arrangements are commonly used for the seawater desalination.

*Corresponding author.

Toward making efficient and low-cost designs of membrane separation processes, the development of mathematical models to predict and optimize the membrane separation performance would be useful [24–28]. The mathematical models developed for any processes could be obtained using two different methods: (1) Theoretical models obtained from solving the governing equations of process [9,16,29]. (2) Empirical models, which is also known as black box modeling, does not need to investigate the mechanisms of the process [20,30–32]. The superiority of the empirical modeling compared to the theoretical models is that it has the possibility to develop quickly the objective function using for process optimization [14]. Moreover, empirical models are more accurate than theoretical ones [33]. However, theoretical models have more generality and once the model is obtained it can be applied to a wide range of problems, but the black box models are usually just applicable to a certain problem and has no generality.

Khayet and Cojocaru [31] developed an artificial neural network model to predict the performance of AGMD process. The air gap thickness, feed temperature, condensation temperature and the flow rate of the feed were considered as input parameters, whereas the objective function was the performance index, which was defined as the permeate flux times the salt rejection. Constructed model could describe the process very well with a linear regression of 0.95 over test data. In similar work [32], they used artificial neural network, to model the sweeping gas membrane distillation process.

Genetic programming (GP) as a branch of genetic algorithm (GA) is a progressive method for repetitively producing nonlinear input–output mathematical expressions in any complex system has been used in a wide variety of applications such as medical, engineering, and etc. [2,34–39]. Suh et al. [40] employed the GP for estimating membrane damage in the membrane integrity test. They used GP as an alternative approach to construct a model to estimate the area of membrane breach while considering other input data (fluorescent nano particle concentration, the pure water permeance and transmembrane pressure). Developed GP models predicted the area of the membrane breach with a good agreement with the experimental data. Shokrkar et al. [37] used GP for modeling the treatment process of oily water by microfiltration membranes, they considered the operating conditions including: concentration, trans-membrane pressure, temperature, and cross-flow velocity as input variables and the permeate flux as the output. They successfully showed that GP is capable to describe the behavior of the system.

In the current study, for the first time we have applied the GP technique for modeling and optimization of the AGMD and WGMD processes. The impact of operating variables on the permeate flux is also investigated which would help to design an economic process. In order to reduce experimental costs, experimental data in the work of Khalifa [17], were used to develop and verifying the GP models. four factors, namely, feed temperature, T_f, feed concentration, C_{feed}, feed flow rate, Q_f and coolant flow rate, Q_c, were considered as input parameters, whereas the objective function was the permeate flux. Predictive models were obtained based on GP, used for optimization of operating conditions.

As mentioned above, Khayet and Cojocaru have used neural network for modeling of AGMD [31], and SGMD [32] processes, successfully. In order to demonstrate the reliability of GP modeling tool in various MD processes, the experimental data of these papers were extracted and modeled by GP and compared to the neural network results. Typically, GP exhibited a higher accuracy than neural network. The results of this comparison are presented in Appendices A, B.

2. Genetic programming (GP)

GP which was introduced by Koza [41] for the first time, is known as extension of the genetic algorithms, but aspect of the system it is much more useful than genetic algorithm. GP is a biologically inspired systematic approach for getting computers to automatically solve a problem, and it is based on natural rules that follow biological evolution [42]. Its mechanism is based on machine learning approach that optimizes a mathematical expression due to a fitness benchmark [41]. GP is known as automatically defined function; it means, it is able to find a mathematical function for a certain problem, automatically [34]. The GP technique is explicit and does not need conceptual designs [43]. Each program in the GP is described by a tree. For example Fig. 1 shows a representation of the function tree for $f(a, b) = \sin(a) + 6*\text{sqrt}(b)$. The binary arithmetic functions, '−', '+' and '*' each have two sub-trees, but mathematical functions such as 'tan', 'sin' and etc. commonly have one sub-tree. In Fig. 1, the connection points are named nodes and regards with the location in the tree, these nodes are divided into two kind as: (1) Internal nodes are called as function; these functions receive one or more input values and produce a single output value (e.g. +, −, ×, sin, cos, exp, etc.) (2) Nodes at the end of arms of tree are called terminal and specify input variables and constant values.

For any problem, it is necessary to specify the five major preparatory steps for the basic version of genetic programming as follows [44]:

The terminal set: A set of input parameters (independent variables).

The function set: A set of specific functions (such as '+', '−', '*', 'sin' and etc.) used in connection with the terminal set to develop solution to the desired problem.

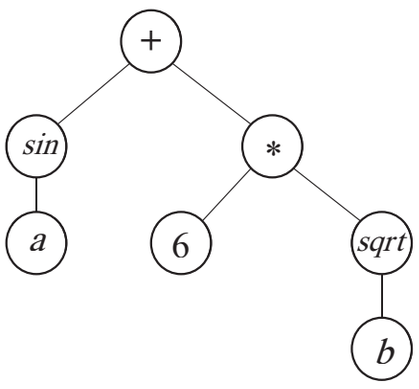

Fig. 1. Sample of a GP tree.

The fitness function: Fitness function evaluates each member of population and determine the difference between predicted results and actual data.

The control parameters: This includes parameters that control the GP process operations.

The termination criterion: This is commonly a predefined number of iteration or a tolerance for the fitness function.

It should be noted that the first three steps determine the area of search for solution, while the final two steps control the quality and speed of the search.

Fig. 2 is a flowchart of GP problem solving approach. The basic mechanism of GP for a specific problem that requires finding a mathematical model is based on a repetitive computational process and can be summarized as follows:

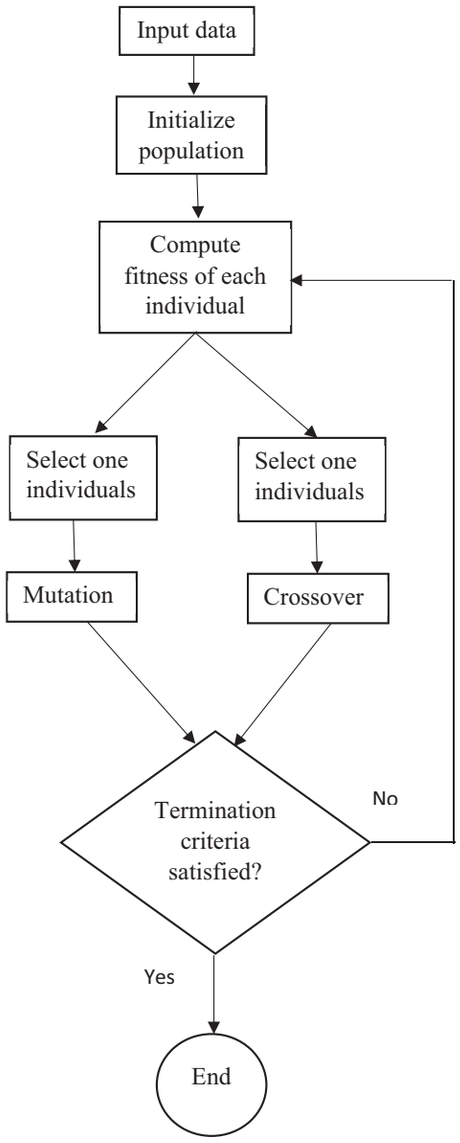

Fig. 2. Solution procedure of GP approach.

(a) Initialization: once loaded the problem data, primary population of programs created randomly.
(b) Fitness evaluation: fitness value, which specify how well the model solves the problem, for the population evaluates.
(c) New generation: new generations of programs are iteratively created by selecting parents based on their fitness and breeding them via genetic operators including crossover, mutation and reproduction.
(d) Termination criteria: when one of the termination criteria; satisfactory fitness or maximum number of generation achieved, the program ends.

Genetic operators introduce variability in the chromosomes and make evolution possible, which may produce better chromosomes in next generations. The function of the crossover operator is to produce new models from two parent models by combination of obtained data from the parents. This operator tries to combine vital components of two expressions in order to create a better mathematical function. However, crossover produces many new offspring, it does not provide any new information into the population, and the population tends to become more and more homogeneous as one begins to dominate. A mutation operator is often introduced to guard against premature convergence. In reproduction, a single model is chosen and a random sub-tree in it is replaced with a freshly generated sub-tree, then that model is placed in the new population. Reproduction is straightforward. It simply copies the chromosome and places it into the new population.

This study applies the GP technique to find a mathematical function for prediction of permeate flux of AGMD and WGMD processes. In this procedure, the fitness function analyses the root mean square error (RMSE) between the value from real data set and that obtained from the model. The terminal is set as [T_f, C_{feed}, Q_f and Q_c], and the functions are set as [+, –, *, /, sin, cos, tan, tanh] and the target responses are: permeate flux for AGMD and WGMD. The fitness function evaluates the root mean square error (RMSE) between the value from original learning data set and that of each chromosome.

3. Data set

The experimental results obtained by Khalifa [17] were used to construct GP models. These experimental data illustrate the permeate flux of MD process under different conditions. The author studied the effects of feed flow rate, feed concentration, feed temperature and the coolant flow rate on the permeate flux in AGMD and WGMD processes. In total, 154 experimental data were obtained. A brief limitation of the model variables has been listed in Table. 1.

4. Results and discussion

4.1. Permeate flux modeling

GP technique which is employed in this study has developed multiple input, single output models as a novel approach in membrane distillation process for prediction

Table 1
Limitation of variables used for GP models construction

Variables	Range
Input variables	
Q_f(L/min)	1–6
C_{feed} (g/L)	0.145–60
T_h (°C)	50–90
Q_c (L/min)	1–4
Output variables	
AGMD permeate flux (kg/m²h)	5–35
WGMD permeate flux (kg/m²h)	14–67

of the permeate flux using an experimental data set that obtained from [17]. This data set provides information about permeate flux under various operating conditions in both membranes configurations: AGMD and WGMD. Two different models were developed for each processes. In total, 154 experimental data were obtained, 75% of all the data were utilized for constructing the models, whereas the remaining were used to evaluate the models. Normalization of data is carried out to construct a more effective GP model for both the model variables and the response. In the present study, the model variables and target (permeate flux) have been normalized before training the models in order to help in the generalization of the GP model. For normalization of the input parameters the below equation was used:

$$z_i = \frac{x_i - x_{\min}}{x_{\max} - x_{\min}} \tag{1}$$

where z_i is the normalized variable while x_i, x_{min} and x_{max} are the actual, minimum and maximum values of parameters, respectively. For normalization of the response data Eq. (2) was used [31,45]

$$Y_i = (1 - \Delta U - \Delta L)\frac{y_i - y_{\min}}{y_{\max} - y_{\min}} \tag{2}$$

where Y_i, y_{min}, and y_{max} indicate the normalized, minimum and maximum values of the response, respectively; ΔU and ΔL are small variations which are considered to define the model limited extrapolation ability (in this study $\Delta U = \Delta L = 0.1$).

In order to find the best model for predicting the processes, 250 generations and 200 populations were considered. The optimum tree depth was 6. Fitness function evaluated the root mean square error (RMSE) of each individual between the experimental values and which is returned by the models. The performance of GP models is illustrated in Fig. 3, the predicted permeate flux is plotted against the experimental value for data used to train the models. The predicted permeate flux in comparison to the experimental results for the test data is shown in Fig. 4. As it can be seen from Figs. 3 and 4, the GP models were capable to predict the permeate flux in a good agreement with the experimental results, for a broad range of operating conditions. The best-so-far GP models that were obtained after satisfying termination criterion for AGMD and WGMD are:

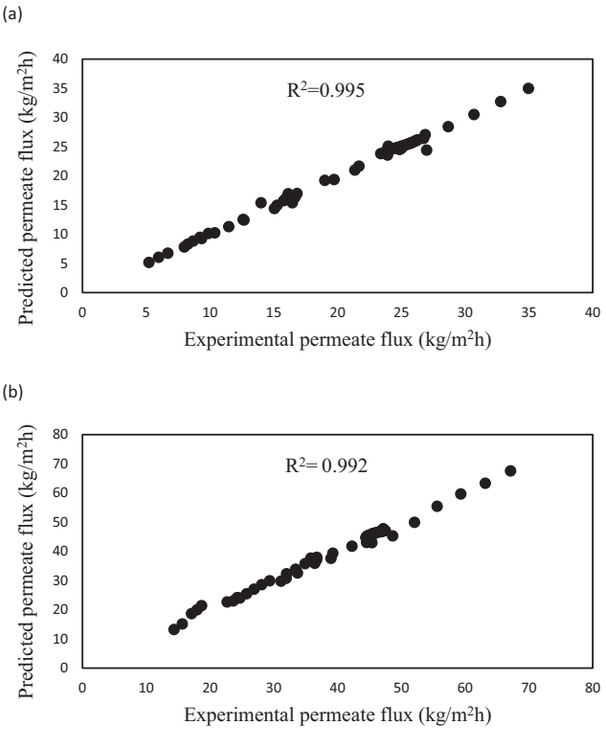

Fig. 3. Predicted permeate flux versus experimental data for training data (a) AGMD, (b) WGMD.

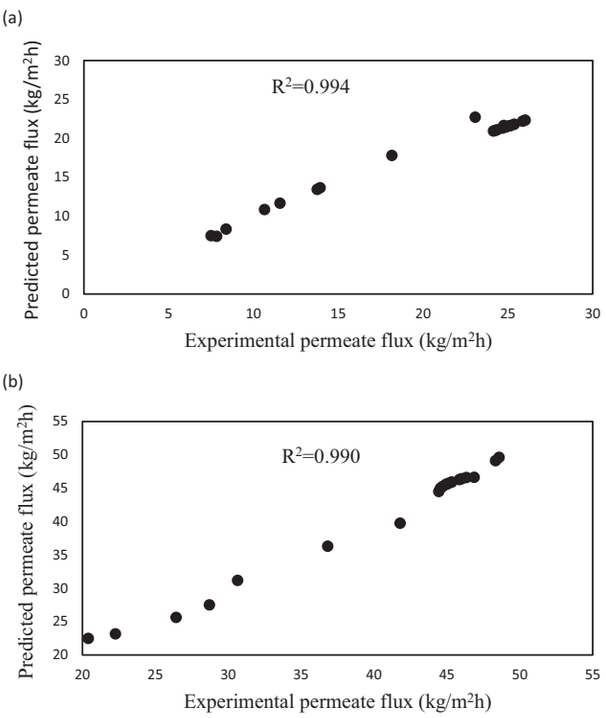

Fig. 4. Predicted permeate flux versus experimental data for test data (a) AGMD, (b) WGMD.

$$y_1 = 0.00629x_1 - 0.2624x_3 + 0.1009\cos((\sin(x_2)x_4^2 + \sin(\tanh(x_1)))$$
$$(x_1 + x_2 + x_3 - \sin(x_1) + 9.744)) + 0.00629\tanh(\exp(x_4))$$
$$-0.2485\cos(\exp(x_4 - x_3) - x_3) + 0.2624\sin(\tanh(x_2)$$
$$-\tanh(\exp(x_4)) + 4.02) + 0.3378\cos(\exp(\exp(-9.917x_1)))$$
$$+0.00629\sin(x_2) + 1.329\sin(x_3) - 0.2624\sin(\exp(x_3)$$
$$-\tanh(x_1)) + 0.3005$$

$$y_2 = 2.796x_1 + 2.796x_2 + 3.703x_3 + 0.07509\sin(\exp(\cos(8.696x_3 + 37.5)))$$
$$-6.24\cos(\cos(x_2)) + 6.24\cos(\sin(x_1)) + 0.1511\cos(6.948x_1)$$
$$+2.796\tanh(x_3) - 6.24\cos(x_2)\sin(x_3) - 0.06221(x_1 - x_3)$$
$$(x_1 - x_3 + x_4 + 4.31) + 0.6514\tanh(x_2\cos(x_1))(2.003\tanh(x_3)$$
$$+6.907)(\sin(\cos(x_1)) + x_4(x_2 - \tanh(6.216x_2))) - 3.155$$

where x_1, x_2, x_3 and x_4 denotes the normalized values of Q_f, C_{feed}, T_f and Q_c respectively, y_1 and y_2 indicate the normalized permeate flux for AGMD and WGMD, respectively. The running time of the GP model development for the reported condition was almost 5 min with Lenovo laptop (Core i5, RAM 6GB, Windows Eight). It should be noted that similar to the artificial neural network [31,32] and response surface methodology [20], GP models are also applicable to a single data set (which used to develop the model) and cannot be used for extrapolation purposes.

In order to demonstrate the validity of the developed models, some statistical parameters, which describes the model performance in estimation of permeate flux, are calculated and presented in Table 2. The formulas for calculating statistical parameters are presented in Ref. [46]. The R-square value illustrates that model results are fitted to the experimental result perfectly. The values of, MSE, SSE, and RMSE show that the proposed models have a little deviation from experimental data.

4.2. Effect of feed temperature

Fig. 5 shows the permeate flux versus the feed temperature at the feed flow rate of 1.5 L/min, feed concentration of 0.145 g/L and the coolant flow rate of 2 L/min, for both AGMD and WGMD configurations. Naturally, as feed temperature increases, the permeate flux tends to increase as well [16,47], hence the models satisfy this expectation very well. Qtaishat et al. [48], reported a similar trend in DCMD configuration, but at higher feed temperatures, their developed model had a few deviations. This deviation was more obvious in the work of Hwang et al. [49]. As it can be shown from Fig. 5, proposed GP models provided good agreement with experimental data for a wide range of feed temperature.

4.3. Effect of feed concentration

As depicted in Fig. 6, the effect of feed concentration on the permeate flux was mathematically modeled and compared to the experimental data. Conditions of this test are: feed flow rate = 1.5 L/min, feed temperature is 70°C and coolant flow rate of 2 L/min. As shown in Fig. 6, the GP models provided excellent prediction for permeate flux. It is illustrated in Fig. 6 that as feed concentration increases, the permeate flux tends to slightly decrease for both AGMD and WGMD, and this is in coherent with published data [50]. Alklaibi and Lior [9] also found a similar trend. A reason for this behavior may be that, increasing the feed concentration causes a decline in the vapor pressure of feed that results in decrease in the driving force. Moreover, it is showed that WGMD has higher permeate flux than AGMD yet.

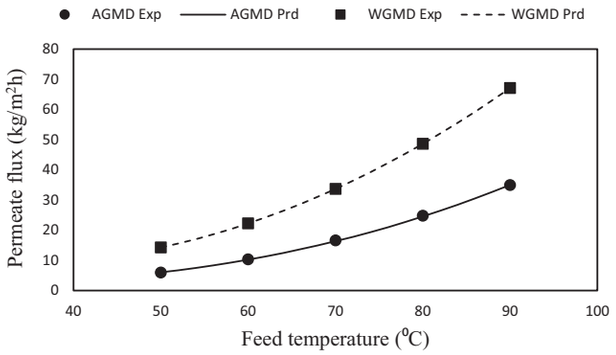

Fig. 5. The effect of feed temperature on the permeate flux for AGMD and WGMD.

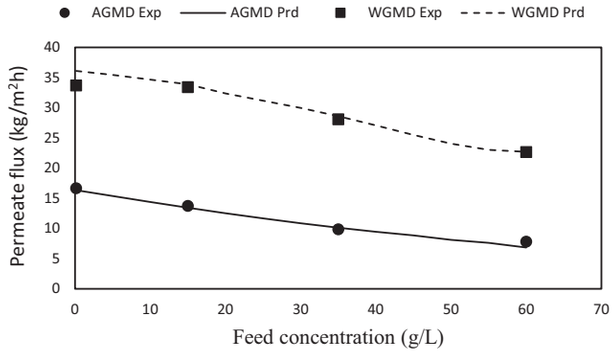

Fig. 6. The effect of feed concentration on the permeate flux for AGMD and WGMD.

Table 2
Statistical parameters of the GP models

Statistical parameter	R^2		SSE		MSE		RMSE		NB%	
MD process	*AGMD*	*WGMD*	*AGMD*	*WGMD*	*AGMD*	*WGMD*	*AGMD*	*WGMD*	*AGMD*	*WGMD*
Training data	0.995	0.992	14.411	57.731	0.253	1.012	0.502814	1.006	–0.134	0.315
Test data	0.994	0.990	1.174	16.103	0.059	0.805	0.242287	0.897	–0.284	0.796

4.4. Effect of feed flow rate

The experimental and predicted permeate fluxes in various feed flow rates and for a concentration of 0.145 g/L, feed temperature of 70°C and coolant flow rate of 2 L/min are presented in Fig. 7. Fig. 7 implies that the GP models showed good coherence with experimental data for both AGMD and WGMD. As it was expected the WGMD has a higher permeate flux than AGMD in the whole of the feed flow rate ranges. It is depicted in Fig. 7, as feed flow rate increases the permeate flux tends to increase, this increment is sharp when the feed flow rate is low and as flow rate increases the permeate flux increases slightly. Similar observation is reported by Chen et al. [51] for a DCMD arrangement, however, in their work there were some errors in prediction of permeate flux as feed flow rate was increasing. In contrary to the most theoretical models GP provided a good prediction about permeate flux for a wide feed flow rate ranges in comparison to the experimental data.

4.5. Flow rate of coolant effects

As depicted in Fig. 8, the effect of the coolant flow rate on the permeate flux was mathematically modeled and compared with the experimental data. Conditions of this test are: feed flow rate = 1.5 L/min and feed temperature is 70°C and feed concentration is 0.145 g/L. However, the coolant flow rate has minimal effect on the permeate flux in both AGMD and WGMD configurations, but as it was expected the coolant flow rate has more effect on the AGMD configuration in comparison to the WGMD. As coolant flow rate increases 400% permeate flux increases only, 14% and 7% for AGMD and WGMD, respectively.

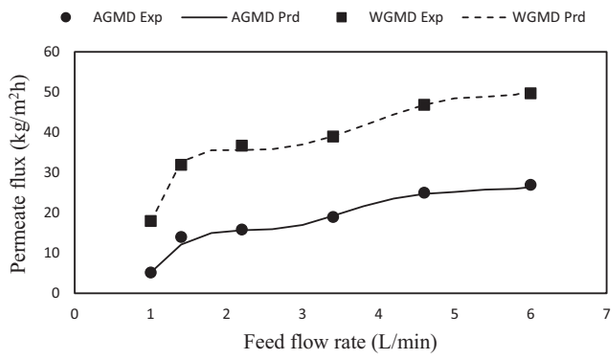

Fig. 7. The effect of feed flow rate on the permeate flux for AGMD and WGMD.

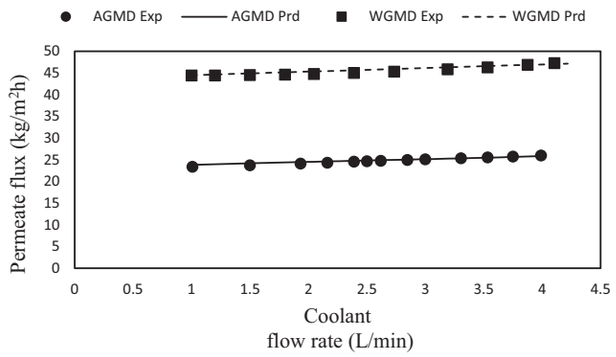

Fig. 8. The effect of coolant flow rate on the permeate flux for AGMD and WGMD.

4.6. Parameter analysis

As mentioned in previous sections the influence of operating parameters on the permeate flux was investigated for both AGMD and WGMD configurations. In this section we are motivated to determine the impact of each operating parameter on the response target. For this purpose, derivative of each curves in Figs. 5–8 were calculated and their average value is reported in Table 3. As it was expected feed concentration has a negative impact on the permeate flux, ie. increasing feed concentration causes a decline in the permeate flux, and in the AGMD configuration, this is more obvious. It can be concluded that feed temperature has a major impact on the permeate flux for both MD arrangements. This kind of information is very useful for designing an economic MD process.

4.7. Process optimization

Theoretically, the highest feed flow rate, highest feed temperature and lowest feed concentration should give the highest permeate flux. However, these parameters may have some interactions with each other. In order to optimize a membrane process, performance index, which is defined as permeate flux times the salt rejection, should be maximized. However, as salt rejection factor in MD processes is close to 100%, permeate flux considered to be maximized.

The simplest way to get the optimum values for the operating conditions is the classical optimization approach. In this method, the derivate of the equation (the expression for the permeate flux which has been obtained in section 4.1) with respect to each variable (x_1, x_2, x_3 and x_4 which refer to Q_f, C_{feed}, T_f and Q_c, respectively) should be calculated separately, the next step is to obtain the roots of these derivative expressions, these roots are considered as the optimum values for each variables (T_f, C_{feed}, Q_f, Q_c). However, this strategy is not suitable to solve very complicated problems in which the objective function is discontinuous, nondifferentiable, or extremely nonlinear. Because the developed GP models are nonlinear, genetic algorithm (GA) method was employed for optimization, instead of the classical approach. GA is capable to solve both constrained and unconstrained optimization problems and it is based on natural selection process that imitates biological evolution for survival of the fittest. The algorithm constantly

Table 3
Growth rate of permeate flux with respect to operating variables

MD process	Variables			
	Q_f	C_{feed}	T_h	Q_c
AGMD	0.619	−0.237	0.779	0.102
WGMD	0.500	−0.166	0.821	0.048

refines a population of individual solutions, which leads to an optimal solution. At each iteration, the genetic algorithm takes individuals at random from the present population and utilizes them as parents to make the children for the next generation. Similar to GP, GA also uses three genetic operators including: crossover, mutation and reproduction to breed the present population. The basic mechanism of GA for a specific optimization problem can be summarized as follows:

1. The algorithm starts by making a random initial population.
2. The algorithm then creates a sequence of new populations from the current one. It uses three genetic operators (crossover, mutation and reproduction) for this matter.
3. The algorithm stops when one of the stopping criteria is reached; either the maximum iteration number is reached or the error becomes smaller than the predefined value.

In this work genetic algorithm toolbox in Matlab software was employed for optimization. Developed GP models for both AGMD and WGMD have been introduced to the software as the objective function which should be maximized.

The computed optimum conditions given by the GP models is summarized in Table 4.

The obtained optimal conditions are within the experimental data limit and as it was expected the higher the feed temperature and lower feed concentration leads to a higher permeate flux but the feed and coolant flow rates are not in their highest value, so it means that these variables have some interaction with each.

5. Conclusions

An important objective of this work was to show the applicability of GP for modeling AGMD and WGMD process for prediction and optimization of the permeate flux. The GP method offers a feasible approach for predicting the permeate flux under different operating condition. The effects of operating factors including feed flow rate, salt concentration, feed temperature and coolant flow rate on the permeate flux were studied, and the gap width was kept fixed for both designs. The results showed a very good agreement with the experimental data in a wide range of operating condition. Feed temperature, T_f and feed flow rate, Q_f were found as the crucial parameters on the process performance. Also it was found that feed concentration and coolant flow has lesser effect on the permeate flux. It was illustrated that, WGMD has higher permeate flux than AGMD particularly in lower feed temperatures. This may be considered as an advantage when developing water gap design in some applications where the maximum feed temperature is limited (eg. Pharmaceutical and food industries). The obtained optimal conditions results in the best process performance are: Q_f = 4.512Lmin, C_{feed} = 0.145 g/L, T_f = 90°C, Q_c = 3.132 L/min with a maximum permeate flux of (38.972 L/m² h and 83.621 L/m² h) for AGMD and WGMD, respectively.

Table 4
Optimal condition for AGMD and WGMD

Operating parameter				Permeate flux (kg/m²h)	
Q_f (L/min)	C_{feed} (g/L)	T_h (°C)	Q_c (L/min)	*AGMD*	*WGMD*
4.512	0.145	90	3.132	38.972	83.621

References

[1] M.M.A. Shirazi, A. Kargari, D. Bastani, L. Fatehi, Production of drinking water from seawater using membrane distillation (MD) alternative: direct contact MD and sweeping gas MD approaches, Desal. Water Treat., 52 (2014) 2372–2381.
[2] A. Asadi Tashvigh, F. Zokaee Ashtiani, A. Fouladitajar, Genetic programming for modeling and optimization of gas sparging assisted microfiltration of oil-in-water emulsion, Desal. Water Treat., 57 (2016) 19160–19170.
[3] A.Asadi Tashvigh, A. Fouladitajar, F.Z. Ashtiani, Modeling concentration polarization in crossflow microfiltration of oil-in-water emulsion using shear-induced diffusion; CFD and experimental studies, Desalination, 357 (2015) 225–232.
[4] Y.M. Manawi, M. Khraisheh, A.K. Fard, F. Benyahia, S. Adham, Effect of operational parameters on distillate flux in direct contact membrane distillation (DCMD): Comparison between experimental and model predicted performance, Desalination, 336 (2014) 110–120.
[5] M.M.A. Shirazi, A. Kargari, M. Tabatabaei, Evaluation of commercial PTFE membranes in desalination by direct contact membrane distillation, Chem. Eng. Process. Process Intensif., 76 (2014) 16–25.
[6] S. Gupta, C.R. Prabha, C. Murthy, Functionalized multi-walled carbon nanotubes/polyvinyl alcohol membrane coated glassy carbon electrode for efficient enzyme immobilization and glucose sensing, J. Environ. Chem. Eng., 4 (2016) 3734–3740.
[7] H. Rabiee, S.M.S. Shahabadi, A. Mokhtare, H. Rabiei, N. Alvandifar, Enhancement in permeation and antifouling properties of PVC ultrafiltration membranes with addition of hydrophilic surfactant additives: Tween-20 and Tween-80, J. Environ. Chem. Eng., 4 (2016) 4050–4061.
[8] M. Norouzi, M. Pakizeh, M. Namvar-Mahboub, The Effect of highly dispersed oxidized multi-walled carbon nanotubes on the performance of PVDF/PVC ultrafiltration membrane, Desal. Water Treat., 57 (2016) 24778–24787.
[9] A. Alklaibi, N. Lior, Membrane-distillation desalination: status and potential, Desalination, 171 (2005) 111–131.
[10] L. Lin, H. Geng, Y. An, P. Li, H. Chang, Preparation and properties of PVDF hollow fiber membrane for desalination using air gap membrane distillation, Desalination, 367 (2015) 145–153.
[11] A. Khalifa, H. Ahmad, M. Antar, T. Laoui, M. Khayet, Experimental and theoretical investigations on water desalination using direct contact membrane distillation, Desalination, 404 (2017) 22–34.
[12] A. Alklaibi, N. Lior, Comparative study of direct-contact and air-gap membrane distillation processes, J. Ind. Eng. Chem. Res., 46 (2007) 584–590.
[13] A. Alsaadi, N. Ghaffour, J.-D. Li, S. Gray, L. Francis, H. Maab, G. Amy, Modeling of air-gap membrane distillation process: a theoretical and experimental study, J. Membr. Sci., 445 (2013) 53–65.
[14] M. Khayet, T. Matsuura, Membrane Distillation: Principles and Applications, Elsevier, 2011.
[15] A. Khalifa, D. Lawal, M. Antar, M. Khayet, Experimental and theoretical investigation on water desalination using air gap membrane distillation, Desalination, 376 (2015) 94–108.

[16] A. Alklaibi, N. Lior, Transport analysis of air-gap membrane distillation, J. Membr. Sci., 255 (2005) 239–253.
[17] A.E. Khalifa, Water and air gap membrane distillation for water desalination – An experimental comparative study, Sep. Purif. Technol., 141 (2015) 276–284.
[18] N. Mokhtar, W. Lau, A. Ismail, W. Youravong, W. Khongnakorn, K. Lertwittayanon, Performance evaluation of novel PVDF–Cloisite 15A hollow fiber composite membranes for treatment of effluents containing dyes and salts using membrane distillation, RSC Adv., 5 (2015) 38011–38020.
[19] A. Alkhudhiri, N. Darwish, N. Hilal, Membrane distillation: A comprehensive review, Desalination, 287 (2012) 2–18.
[20] A.E. Khalifa, D.U. Lawal, Application of response surface and Taguchi optimization techniques to air gap membrane distillation for water desalination—A comparative study, Desal. Water Treat., 57 (2016) 28513–28530.
[21] F.A. Banat, J. Simandl, Desalination by membrane distillation: A parametric study, Sep. Sci. Technol., 33 (1998) 201–226.
[22] G. Meindersma, C. Guijt, A. De Haan, Desalination and water recycling by air gap membrane distillation, Desalination, 187 (2006) 291–301.
[23] A.A. AlcheikhHamdon, N.A. Darwish, N. Hilal, The use of factorial design in the analysis of air-gap membrane distillation data, Desalination, 367 (2015) 90–102.
[24] Q.-F. Liu, S.-H. Kim, Evaluation of membrane fouling models based on bench-scale experiments: a comparison between constant flowrate blocking laws and artificial neural network (ANNs) model, J. Membr. Sci., 310 (2008) 393–401.
[25] K.-J. Hwang, C.-Y. Liao, K.-L. Tung, Analysis of particle fouling during microfiltration by use of blocking models, J. Membr. Sci., 287 (2007) 287–293.
[26] S.M.G. Demneh, B. Nasernejad, H. Modarres, Modeling investigation of membrane biofouling phenomena by considering the adsorption of protein, polysaccharide and humic acid, Colloids Surf., B Colloids Surf., B, 88 (2011) 108–114.
[27] H. Moshiri, B. Nasernejad, H. Ale Ebrahim, M. Taheri, Solution of coupled partial differential equations of a packed bed reactor for SO_2 removal by lime using the finite element method, RSC Adv., 5 (2015) 18116–18127.
[28] G. Rao, S.R. Hiibel, A. Achilli, A.E. Childress, Factors contributing to flux improvement in vacuum-enhanced direct contact membrane distillation, Desalination, 367 (2015) 197–205.
[29] A. Alklaibi, The potential of membrane distillation as a standalone desalination process, Desalination, 223 (2008) 375–385.
[30] A. Shahsavand, M.P. Chenar, Neural networks modeling of hollow fiber membrane processes, J. Membr. Sci., 297 (2007) 59–73.
[31] M. Khayet, C. Cojocaru, Artificial neural network modeling and optimization of desalination by air gap membrane distillation, Sep. Purif. Technol., 86 (2012) 171–182.
[32] M. Khayet, C. Cojocaru, Artificial neural network model for desalination by sweeping gas membrane distillation, Desalination, 308 (2013) 102–110.
[33] I. Hitsov, T. Maere, K. De Sitter, C. Dotremont, I. Nopens, Modelling approaches in membrane distillation: A critical review, Sep. Purif. Technol., 142 (2015) 48–64.
[34] T.-M. Lee, H. Oh, Y.-K. Choung, S. Oh, M. Jeon, J.H. Kim, S.H. Nam, S. Lee, Prediction of membrane fouling in the pilot-scale microfiltration system using genetic programming, Desalination, 247 (2009) 285–294.
[35] A. Nazari, S. Riahi, Computer-aided Prediction of the ZrO_2 nanoparticles' effects on tensile strength and percentage of water absorption of concrete specimens, J. Mater. Sci. Technol., 28 (2012) 83–96.
[36] M.R. Karahroudi, S.M. Shirazi, K. Sepanloo, Optimization of designing the core fuel loading pattern in a VVER-1000 nuclear power reactor using the genetic algorithm, Ann. Nucl. Energy, 57 (2013) 142–150.
[37] H. Shokrkar, A. Salahi, N. Kasiri, T. Mohammadi, Prediction of permeation flux decline during MF of oily wastewater using genetic programming, Chem. Eng. Res. Des., 90 (2012) 846–853.
[38] A.Asadi Tashvigh, F.Z. Ashtiani, M. Karimi, A. Okhovat, A novel approach for estimation of solvent activity in polymer solutions using genetic programming, Calphad, 51 (2015) 35–41.
[39] M. Karimi, A. Asadi Tashvigh, F. Asadi, F.Z. Ashtiani, Determination of concentration-dependent diffusion coefficient of seven solvents in polystyrene systems using FTIR-ATR technique: experimental and mathematical studies, RSC Adv., 6 (2016) 9013–9022.
[40] C. Suh, B. Choi, S. Lee, D. Kim, J. Cho, Application of genetic programming to develop the model for estimating membrane damage in the membrane integrity test using fluorescent nanoparticle, Desalination, 281 (2011) 80–87.
[41] J.R. Koza, Genetic programming: on the programming of computers by means of natural selection, MIT press, 1992.
[42] J.R. Koza, R. Poli, Genetic Programming, in: E.K. Burke, G. Kendall (Eds.) Search Methodologies: Introductory Tutorials in Optimization and Decision Support Techniques, Springer US, Boston, MA, 2005, pp. 127–164.
[43] A. Fouladitajar, F.Z. Ashtiani, A. Okhovat, B. Dabir, Membrane fouling in microfiltration of oil-in-water emulsions; a comparison between constant pressure blocking laws and genetic programming (GP) model, Desalination, 329 (2013) 41–49.
[44] M.J. Willis, H.G. Hiden, P. Marenbach, B. McKay, G.A. Montague, Genetic programming: an introduction and survey of applications, in: Second International Conference On Genetic Algorithms In Engineering Systems: Innovations And Applications, 1997, pp. 314–319.
[45] B. Sarkar, A. Sengupta, S. De, S. DasGupta, Prediction of permeate flux during electric field enhanced cross-flow ultrafiltration—a neural network approach, Sep. Purif. Technol., 65 (2009) 260–268.
[46] A. Okhovat, S.M. Mousavi, Modeling of arsenic, chromium and cadmium removal by nanofiltration process using genetic programming, Appl. Soft Comput., 12 (2012) 793–799.
[47] A. Alklaibi, N. Lior, Heat and mass transfer resistance analysis of membrane distillation, J. Membr. Sci., 282 (2006) 362–369.
[48] M. Qtaishat, T. Matsuura, B. Kruczek, M. Khayet, Heat and mass transfer analysis in direct contact membrane distillation, Desalination, 219 (2008) 272–292.
[49] H.J. Hwang, K. He, S. Gray, J. Zhang, I.S. Moon, Direct contact membrane distillation (DCMD): Experimental study on the commercial PTFE membrane and modeling, J. Membr. Sci., 371 (2011) 90–98.
[50] V. Calabro, B.L. Jiao, E. Drioli, Theoretical and experimental study on membrane distillation in the concentration of orange juice, J. Ind. Eng. Chem. Res., 33 (1994) 1803–1808.
[51] T.-C. Chen, C.-D. Ho, H.-M. Yeh, Theoretical modeling and experimental analysis of direct contact membrane distillation, J. Membr. Sci., 330 (2009) 279–287.

Appendix A

$$y = 0.1385x_1 - 0.1287x_3 + 3.092\exp(-0.1758\cos(x_2x_4)) + 7.712\cos(\sin(x_1)) + 6.522\tanh(\sin(\cos(\cos(x_1 - x_2)))) - 0.4813\cos(x_1 - x_4 + \cos(x_3) - \sin(x_1) + \tanh(x_3) + 0.0024) - 0.1893\exp(\cos(\cos(x_2^2 - x_1)) - \cos(x_1) + si(x_3)) + 0.00825\sin(x_1 + 0.9754) - 0.5482\tanh(\cos(\tanh(x_2) - x_1x_2^2)) - 0.4813\sin(x_3x_4 - 4.947) - 0.005603x_2(9.633x_1 + x_3 + \exp(\cos(x_1)) + \tanh(x_1)) + 0.00825x_1x_4 + 0.01299x_2^2 + 0.1287\sin(\cos(x_1x_2))\tanh(\sin(\tanh(x_2)) - x_4 - x_2 + \tanh(x_1))(\tanh(x_3) + \cos(x_1 - 8.349)) - 13.05$$

x_1: A, x_2: T_f, x_3: T_c, x_4: Q, y: Permeate flux.

Table A.1
Experimental data for AGMD process from Ref. [31]

Input variables				Flux	GP model
A (mm)	T_f (°C)	T_c (°C)	Q (L/h)	y (kg/m²h)	y (kg/m²h)
3	70	25	200	45.487	44.55897
3	70	15	200	50.232	49.75071
3	60	25	200	30.185	29.77823
3	60	15	200	35.264	34.6058
3	70	25	150	43.959	43.11001
3	70	15	150	47.468	47.6298
3	60	25	150	29.288	29.21906
3	60	15	150	34.279	33.37467
3	65	26.1	175	34.42	34.19406
3	65	13.9	175	39.997	40.03531
3	71	20	175	45.382	45.87081
3	59	20	175	29.264	28.30934
3	65	20	205	37.837	38.05299
3	65	20	145	36.855	36.88464
3	65	20	175	36.85	36.98495
4.2	70	25	200	38.951	38.46393
4.2	70	15	200	43.345	42.63955
4.2	60	25	200	26.629	25.96124
4.2	60	15	200	29.039	29.54689
4.2	70	25	150	35.349	36.33258
4.2	70	15	150	39.079	39.92976
4.2	60	25	150	24.461	24.71967
4.2	60	15	150	25.642	27.72689
4.2	65	26.1	175	29.569	29.73678
4.2	65	13.9	175	34.681	35.31849
4.2	71	20	175	41.648	41.98409
4.2	59	20	175	24.82	25.4775
4.2	65	20	205	34.52	34.60547
4.2	65	20	145	31.277	31.14287
4.2	65	20	175	33.528	32.4061
7.4	70	25	200	31.565	32.01301
7.4	70	15	200	36.866	36.79917
7.4	60	25	200	20.964	21.48601
7.4	60	15	200	25.941	25.68948
7.4	70	25	150	27.81	28.68772
7.4	70	15	150	32.675	32.63901
7.4	60	25	150	19.626	19.0505
7.4	60	15	150	23.776	22.41909
7.4	65	26.1	175	25.651	24.66011
7.4	65	13.9	175	29.547	30.48146
7.4	71	20	175	34.284	34.7827
7.4	59	20	175	20.444	21.53551
7.4	65	20	205	28.481	29.78197
7.4	65	20	145	25.547	25.0705
7.4	65	20	175	26.905	27.4722
3	30	20	175	3.147	3.993917
3	40	20	175	9.189	8.272396
3	50	20	175	17.669	18.54953
4.2	30	20	175	2.827	2.310808
4.2	40	20	175	7.898	7.658679
4.2	50	20	175	16.406	15.40362
7.4	30	20	175	2.039	2.427773
7.4	40	20	175	5.613	5.916667
7.4	50	20	175	12.159	12.99068
3	70	20	200	45.273	45.98672
3	65	15	150	38.738	39.4845
3	65	25	200	34.238	35.96185
3	60	15	175	32.151	33.59277
4.2	70	20	200	40.507	39.9004
4.2	65	15	150	34.198	33.77528
4.2	65	25	200	32.505	32.07832
4.2	60	15	150	29.622	27.72689
7.4	70	20	200	34.931	34.46156
7.4	65	15	150	27.642	27.60795
7.4	65	25	200	27.855	26.72604
7.4	60	15	175	24.025	23.65339
3	71	13.9	205	51.075	50.34009
3	63	13.9	205	37.111	36.74585
4.2	71	13.9	205	47.289	47.64093
4.2	63	13.9	205	35.039	35.78124
7.4	71	13.9	205	40.938	40.72187
7.4	63	13.9	205	32.898	31.41694

Table A.2
Comparison between neural networks and GP

Data set	R^2	
	Neural network from Ref. [31]	GP model
Training data	0.9965	0.9961
Validating data	0.9483	0.9767
Test data	0.9493	0.9885

Appendix B

$$y = 0.0257\cos(\sin(x_1 - x_2)) - 0.05542\cos(x_1(x_2 - 3x_1 + \cos(x_2) + x_1x_3))$$
$$\_0.02871\sin(\sin(\sin(x_1) + \tanh(x_2)) + \tanh(x_2) + \tanh(x_3)$$
$$-2x_3(x_1 - 1.946)) - 0.0257\tanh(\cos(x_2) + \tanh(x_3))$$
$$-0.0257\cos(2.96x_1x_2(x_2 + x_3 - \sin(x_1))) - 18.46\cos(\cos(\tanh(x_2)))$$
$$-1.204\tanh(\cos(2x_2))(x_2 + \tanh(\tanh(x_3))) + 0.01492x_1x_2$$
$$+0.2616\sin(\sin(x_1) + \cos(x_1)\tanh(1x) + 6.833)\cos(x_2 + x_3) + 12.92$$

x_1: T_f, x_2: U_a, x_3: U_w, y: Permeate flux.

Table B.1
Experimental data from Ref [32]

Input variables			Flux	GP model
T_f (°C)	U_a (m/s)	U_w (m/s)	J (kg/m²h)*10⁻³	J (kg/m²h)*10⁻³
68	1.932	0.2	1.106	1.1085
54	1.932	0.2	0.636	0.694664
68	0.966	0.2	0.65	0.615143
54	0.966	0.2	0.459	0.444998
68	1.932	0.14	0.969	0.970204
54	1.932	0.14	0.74	0.699402
68	0.966	0.14	0.582	0.572325
54	0.966	0.14	0.326	0.323418
70	1.449	0.17	1.016	1.021619
52	1.449	0.17	0.499	0.53395
61	2.028	0.17	0.841	0.84619
61	0.869	0.17	0.499	0.513087
61	1.449	0.206	0.989	0.789927
61	1.449	0.134	0.634	0.669004
61	1.449	0.17	0.67	0.784802
68	1.449	0.17	0.919	0.91487
54	1.449	0.17	0.542	0.540941
65	1.884	0.17	0.988	0.908319
58	1.014	0.17	0.528	0.539457
65	1.014	0.17	0.647	0.623989
58	1.884	0.17	0.698	0.675115
65	1.594	0.194	0.849	0.910218
58	1.304	0.146	0.78	0.704337
65	1.304	0.146	0.626	0.657286
61	1.738	0.146	0.893	0.857911
58	1.594	0.194	0.686	0.731417
61	1.159	0.194	0.61	0.614508
54	0.966	0.17	0.361	0.354406
68	0.966	0.17	0.579	0.600088
54	1.932	0.17	0.679	0.660409
68	1.932	0.17	1.024	1.08174
54	1.449	0.14	0.549	0.547809
68	1.449	0.14	0.846	0.855928
54	1.449	0.2	0.562	0.606213
68	1.449	0.2	0.966	0.95881
61	0.966	0.14	0.473	0.468192
61	1.932	0.14	0.896	0.935827
61	0.966	0.2	0.409	0.493856
61	1.932	0.2	0.804	0.841409
65	1.69	0.185	0.956	0.973742
57	1.69	0.185	0.688	0.720706
65	1.207	0.185	0.704	0.732976
57	1.207	0.185	0.543	0.607479
65	1.69	0.155	0.873	0.860497
57	1.69	0.155	0.639	0.628444
65	1.207	0.155	0.6	0.633407
57	1.207	0.155	0.559	0.516849
66	1.449	0.17	0.887	0.911478
56	1.449	0.17	0.625	0.633561
61	1.738	0.17	0.993	0.970701
61	1.159	0.17	0.552	0.564909
61	1.449	0.188	0.802	0.760207
61	1.449	0.152	0.664	0.728292

Table B.2
Comparison between neural networks and GP

Data set	R^2	
	Neural network from [32]	GP model
Training, validation and test data	0.8	0.9372
Validating data	0.93	0.9

For more description about nomenclatures which used in appendices, readers are referred to [31,32].